Published in final edited form as:
Neuroscience. 2009 March 3; 159(1): 104–114. doi:10.1016/j.neuroscience.2008.11.052.

Intracellular Zn^{2+} increases contribute to the progression of excitotoxic Ca^{2+} increases in apical dendrites of CA1 pyramidal neurons

T.A. Vander Jagt[1], **J.A. Connor**[1], **J.H. Weiss**[2], and **C.W. Shuttleworth**[1]

1*Department of Neurosciences, University of New Mexico School of Medicine, Albuquerque NM 87131*

2*Departments of Neurology & Anatomy and Neurobiology, University of California Irvine, Irvine, CA 92697*

Abstract

Sustained intracellular Ca^{2+} elevation is a well-established contributor to neuronal injury following excessive activation of NMDA-type glutamate receptors. Zn^{2+} can also be involved in excitotoxic degeneration, but the relative contributions of these two cations to the initiation and progression of excitotoxic injury is not yet known. We previously concluded that extended NMDA exposure led to sustained Ca^{2+} increases that originated in apical dendrites of CA1 neurons and then propagated slowly throughout neurons and caused rapid necrotic injury. However the fluorescent indicator used in those studies (Fura-6F) may also respond to Zn^{2+}, and in the present work we examine possible contributions of Zn^{2+} to indicator signals and to the progression of degenerative signaling along CA1 dendrites. Selective chelation of Zn^{2+} with N,N,N′,N′-tetrakis(2-pyridylmethyl)ethylenediamine (TPEN) significantly delayed, but did not prevent the development and progression of sustained high-level Fura-6F signals from dendrites to somata. Rapid indicator loss during the Ca^{2+} overload response, which corresponds to rapid neuronal injury, was also not prevented by TPEN. The relationship between cytosolic Zn^{2+} and Ca^{2+} levels was assessed in single CA1 neurons co-loaded with Fura-6F and the Zn^{2+}-selective indicator FluoZin-3. NMDA exposure resulted in significant initial increases in FluoZin-3 increases that were prevented by TPEN, but not by extracellular Zn^{2+} chelation with Ca-EDTA. Consistent with this result, Ca-EDTA did not delay the progression of Fura-6F signals during NMDA. Removal of extracellular Ca^{2+} reduced, but did not prevent FluoZin-3 increases. These results suggest that sustained Ca^{2+} increases indeed underlie Fura-6F signals that slowly propagate throughout neurons, and that Ca^{2+} (rather than Zn^{2+}) increases are ultimately responsible for neuronal injury during NMDA. However, mobilization of Zn^{2+} from endogenous sources leads to significant neuronal Zn^{2+} increases, that in turn contribute to mechanisms of initiation and progression of progressive Ca^{2+} deregulation.

Keywords

Hippocampal slice; FluoZin-3; Fura; TPEN; NMDA

Please address correspondence to: C. William Shuttleworth, Ph.D., Department of Neurosciences, University of New Mexico School of Medicine, MSC08 4740, 1 University of New Mexico, Albuquerque, NM 87131, E-mail: E-mail: bshuttleworth@salud.unm.edu, Phone: 505-272-4290, Fax: 505-272-8082.

Introduction

There has been longstanding interest in neuronal Ca^{2+} loading following both normal and excessive glutamate receptor activation, with much evidence demonstrating that sustained Ca^{2+} accumulation can trigger neuronal injury in a variety of experimental models (Choi, 1988; Nicholls and Budd, 2000; Connor and Shuttleworth, 2001; Arundine and Tymianski, 2003). Zn^{2+} is also present at significant concentrations in the brain, and can contribute to neuronal death following its mobilization from synaptic vesicles and/or intracellular binding sites (Choi and Koh, 1998; Weiss et al., 2000; Frederickson et al., 2005). At present there is controversy over the relative importance of each ion in the complex reactions that initiate neuronal injury. We therefore considered it an important goal to determine the extent to which Ca^{2+}- and Zn^{2+}-dependent mechanisms may interact to initiate neuronal injury.

In an effort to test the roles of Ca^{2+} in initiation of excitotoxic injury, we recently used a low-affinity Ca^{2+}-sensitive indicator (Fura-6F) to examine responses of CA1 neuron dendrites during extended exposures to NMDA. We concluded that very large Ca^{2+} increases originated in distal CA1 apical dendrites and propagated slowly throughout the neuron and arrival of sustained Ca^{2+} elevations at somata triggered relatively rapid cell injury (Dietz et al., 2007; Vander Jagt et al., 2008). Indicators of the Fura family are also highly sensitive to Zn^{2+} with affinities, in vitro, higher than for Ca^{2+} (e.g. Grynkiewicz et al., 1985; Hechtenberg and Beyersmann, 1993; Simons, 1993; Atar et al., 1995; Sensi et al., 1997; Cheng and Reynolds, 1998; Martin et al., 2006). When measured against physiological Ca^{2+} concentrations in intact neurons, the apparent sensitivity of Fura indicators for Zn^{2+} is greatly decreased (Marchi et al., 2000; Devinney et al., 2005) and Ca^{2+} and Zn^{2+} signals can be effectively discriminated (Devinney et al., 2005; Dietz et al., 2008). However, it is not yet known whether Zn^{2+} binding to the indicator could contribute to the very large Fura-6F signals observed to propagate along CA1 dendrites and furthermore whether Zn^{2+} increases could contribute to mechanisms triggering Ca^{2+} deregulation.

Previous studies of cell culture neurons have established that glutamate receptor activation in the presence of exogenous Zn^{2+} can lead to intracellular Zn^{2+} increases and toxicity, as a result of influx through channels and transporters that are better known for their flux of Ca^{2+} (Weiss et al., 1993; Sensi et al., 1997; Choi and Koh, 1998; Weiss et al., 2000). Zn^{2+} can also bind to NMDA receptors and inhibit function (Peters et al., 1987; Westbrook and Mayer, 1987) but also directly permeates the channel, although the process is relatively slow and can appear as a flicker-type block of channel activity (Christine and Choi, 1990). Exposure to NMDA could also lead to Zn^{2+} influx via other channels as a secondary consequence of depolarization during NMDA exposure, for example voltage-dependent Ca^{2+} channels, or possibly reverse-operation of sodium calcium exchangers (Sensi et al., 1997; Choi and Koh, 1998; Weiss et al., 2000). Zn^{2+} can be present in the extracellular space as a result of contaminant from solution preparation (Kay, 2004), but there is also evidence that significant amounts of endogenous Zn^{2+} are released in the CA1 region following stimulation of Schaffer collateral fibers in murine hippocampal slices (Qian and Noebels, 2006). In addition to influx from the extracellular space, Zn^{2+} can also be mobilized from intracellular binding proteins following excitotoxic or oxidative stress (Aizenman et al., 2000; Lee et al., 2003; Bossy-Wetzel et al., 2004) and it is possible that one or both sources of Zn^{2+} could be mobilized following extended NMDA exposures in slice.

The present study measured Zn^{2+} dynamics in single CA1 neurons in murine hippocampal slices during extended NMDA exposures, using combinations of fluorescent indicators and Zn^{2+}-selective chelators in order to probe for possible contributions of Zn^{2+} accumulation to subsequent Ca^{2+} deregulation and neuronal damage. Some of these results have been presented in Abstract form (Vander Jagt et al., 2007).

Experimental Procedures

Animals

Male FVB/N mice were obtained from Harlan (Bar Harbor, Maine) at 4 weeks of age and housed under standard conditions (12hr/12hr light/dark cycle) before sacrifice at 4-6 weeks of age. Mice were deeply anesthetized with a mixture of ketamine and xylazine (85mg/ml and 15mg/ml, respectively; 150μl s.c.) and decapitated. Brains were quickly removed and placed in ice cold cutting solution (see below for composition). Experiments were carried out in accordance with the National Institute of Health guidelines for the humane treatment of laboratory animals, and the protocol for these procedures was reviewed annually by the Institutional Animal Care and Use Committee at the University of New Mexico School of Medicine.

Slice Preparation and single-cell indicator loading

The procedures for slice preparation and loading of fluorescent indicators were identical to those recently described (Vander Jagt et al., 2008) and are summarized here. A Vibratome (St. Louis, MO) was used to prepare coronal slices (350μm), which were then warmed to 35°C for 1 hour and then held at room temperature until used for recording. Recordings were made on a fixed stage microscope (Olympus BX51WI) with a Warner Instruments recording chamber (RC-27L) and slices were superfused with warmed (32°C), oxygenated ACSF at 2-2.5 ml/min. Single CA1 neurons were visualized by using DIC optics and briefly loaded with fluorescent indicators via patch pipettes in the "whole-cell" recording mode. As previously described, neurons were used for analysis only if the current required to maintain a holding voltage of -70 mV exceeded was <100pA and membrane resistance was between 100 and 250MΩ. In studies of cells loaded with Fura-6F alone, 1mM indicator was included in the pipette solution (Vander Jagt et al., 2008) and for experiments co-loading FluoZin-3 and Fura-6F, initial pipette indicator concentrations were 0.6mM and 0.5mM, respectively. After obtaining whole-cell access, indicator loading was strictly limited to 3 minutes to minimize loss of diffusible cellular components and final cellular indicator concentrations in neurons was estimated at ≤ 200μM (see Vander Jagt et al., 2008). Loading pipettes were then carefully removed, and cells were discarded if soma Ca^{2+} elevations were detected during the pipette removal process. Cells were then allowed to recover for 25 minutes after pipette removal before NMDA challenge.

Imaging

Fluorescence data were captured using a CCD-based system (Till Imago SensiCam, Polychrome IV monochrometer, TillVision v4.1 software, Till Photonics Pleasanton, CA). In studies of Fura-6F alone, indicator was excited at 350/380nm (25-50ms) and emission detected with a 400nm / 510±40nm dichromatic mirror / emission filter combination. Co-loaded neurons were excited sequentially at 350/380/490nm, (100-150ms) and emission of both indicators detected with a single dichromatic mirror / emission filter set (505nm / 535±25nm), similar to previous reports (Devinney et al., 2005; Dietz et al., 2008). Acquisition rate was 0.2Hz for each indicator (single image or image pair). Fura-6F ratios were converted to estimated Ca^{2+} concentrations, using procedures previously described (Vander Jagt et al., 2008) and data for FluoZin-3 was presented as $\Delta F/F_0$ after background subtraction, except where noted.

Reagents and Solutions

ACSF contained (in mM): 126 NaCl, 2 KCl, 1.25 NaH_2PO_4, 1 $MgSO_4$, 26 $NaHCO_3$, 2 $CaCl_2$, and 10 glucose, equilibrated with 95%O_2 / 5%CO_2. Slice cutting solution contained (in mM): 2 KCl, 1.25 NaH_2PO_4, 6 $MgSO_4$, 26 $NaHCO_3$, 0.2 $CaCl_2$, 10 glucose, 220 sucrose and 0.43 ketamine. Cutting and recording solutions were all 315-320 mOsmol. Whole-cell ppipette solutions contained (in mM): 135 K-gluconate, 8 NaCl, 1 MgCl2, 10 HEPES, 2 Mg^{2+}-ATP

and was pH (7.25) adjusted with KOH. NMDA exposures were made in modified ACSF lacking added Mg^{2+} and supplemented with nimodipine (10μM), as described in (Vander Jagt et al., 2008). Fluorescent indicators were from Invitrogen-Molecular Probes (Eugene, OR) and other reagents were from Sigma Chemical Co. (St. Louis, MO). Nimodipine was prepared in ethanol (10mM stock) and NMDA stocks were prepared in de-ionized water (5mM) and stored at -20°C until use. Two Zn^{2+}-selective chelators were used: N,N,N′,N′-Tetrakis (2-pyridylmethyl) ethylenediamine (TPEN) which has $K_D(Zn^{2+}) = 2.95\times10^{-16}$M and $K_D(Ca^{2+})$ of 4.0×10^{-5} (Arslan et al., 1985) and Ca-EDTA, which exchanges its bound Ca^{2+} for Zn^{2+} with a K_D of 8×10^{-14}M (Lee et al., 2002). TPEN was prepared fresh prior to each use in DMSO (50mM) and Ca-EDTA was prepared in ACSF. Tests of possible effects of matched vehicle DMSO concentrations (max 0.1%) showed no effects on NMDA-stimulated responses in these experiments.

Statistics

Group data are presented as mean±SEM, and "n" values refer to the number of neurons examined. Only one neuron was studied in each slice. For each experimental condition, no more than two slices were examined from a single animal. Differences between group data were analyzed with unpaired Student's t-tests, with $p<0.05$ being considered significant. Each set of experiments presented was internally controlled, using similar numbers of control slices from interleaved experiments to compare with each experimental condition. This was important to control for possible differences in animals, tissue handling or other unknown variables that may contribute to small changes in average response times.

Results

1. Effects of Zn^{2+} chelation with TPEN on overall Fura-6F responses

Figure 1A shows the characteristic responses of a single CA1 neuron to extended NMDA exposure, monitored using the low-affinity indicator Fura-6F. As previously described (Dietz et al., 2007; Vander Jagt et al., 2008), the Fura-6F signal showed an initial spike followed by recovery to near-baseline for about 25 min and then a larger and sustained increase originating in the distal dendrite that propagated slowly and invaded the soma. Arrival of the sustained response at the soma was accompanied by rapid loss of indicator, suggesting acute neuronal injury (see below). Figure 1B shows a neuron from the same experimental group, but in this case the membrane-permeable, Zn^{2+}-selective chelator, TPEN was present throughout (50μM; with 20 min pre-exposure). Although TPEN did have significant quantitative effects (see below), it did not change the basic characteristics of the compound Fura-6F response. There was still an initial Fura-6F spike ~6 min after NMDA onset, followed by recovery to near-baseline levels. In TPEN, the propagating sustained Fura-6F increase was still sufficiently large to saturate the indicator, and progressed apparently normally along the apical dendrite to the soma. This result, when taken together with previous observations that Fura-6F signals were abolished by extracellular Ca^{2+} removal, implies that Ca^{2+} (rather than Zn^{2+}) increases are primarily responsible for the large propagating Fura-6F signals associated with neuronal degeneration. Figure 2A shows recordings from a group of experiments with and without TPEN, and reveals that TPEN produced a significant decrease in amplitude of the initial spikes, and a consistent delay in the arrival of dendritic Ca^{2+} overload responses at somata.

2. Effects of TPEN on initial Fura-6F spikes

Initial Fura-6F spikes were significantly decreased (15.3±2.8 vs. 5.5±1.8μM, control and TPEN respectively; $p<0.01$, n=6,7), but there was no difference in the latency of these initial events (7.9±0.3 vs. 8.2±0.5min; control and TPEN respectively; $p=0.6$, n=6,7).

While TPEN has a very high affinity for Zn^{2+} (K_D 2.9×10^{-16}M), it still binds Ca^{2+} (K_D 4×10^{-5}M (Arslan et al., 1985)), and it is possible that 50μM TPEN could buffer intracellular Ca^{2+} levels and thereby decrease initial Fura-6F spike responses. This seems unlikely since when we reduced the TPEN concentration to 10μM, there was still a very similar reduction of initial spike amplitude (15.1±2.6 vs. 6.7±1.8μM, control and 10μM TPEN respectively, p=0.03, n=6 each) which would not be expected if Ca^{2+} buffering were the main effect. Given evidence that intracellular Zn^{2+} increases occurs at the same time (see below), it seems more likely that Zn^{2+} binding to Fura-6F or downstream consequences of Zn^{2+} mobilization modulates the initial Fura-6F spikes.

3. Effects of TPEN on propagating Ca^{2+} overload responses

The average time taken for Ca^{2+} overload to reach the soma after NMDA application (see Fig 2A) was significantly increased by TPEN (45.5±2.2 vs. 63.9±2.7min, control and TPEN respectively, $p<0.01$, n=6,7). This increase was not related to the differences in the initial spike, since it has been shown that abolishing the spike altogether with transient removal of extracellular Ca^{2+} did not influence the timing of dendritic Ca^{2+} deregulation (Vander Jagt et al., 2008b). This was confirmed in a set of experiments where TPEN was applied immediately after the initial spike responses, instead of pre-exposing slices to the chelator. Under these conditions, there was still a significantly increased delay in arrival of Ca^{2+} overload responses at somata (38.6±3.4 vs. 54.1±4.3min, control and TPEN respectively; $p<0.02$, n=6,7). The effect here was smaller than in slices pre-exposed to the chelator, and this is presumably due to fact that it takes some time for the chelator to accumulate to effective concentrations in neurons in slice, while activation of deleterious processes by NMDA is already ongoing.

When measured at the isobestic point for Ca^{2+} (360nm), loss of Fura-6F fluorescence can provide an effective measure of acute membrane failure, as the charged indicator of 836 MW is rapidly lost from the loaded cell after Ca^{2+} overload occurs ((Vander Jagt et al., 2008) and see also (Randall and Thayer, 1992)). TPEN did not modify this injury response, following invasion of somata by Ca^{2+} overload responses. Figure 2C shows Fura-6F fluorescence loss associated with sustained Ca^{2+} increases in the presence of TPEN. Indicator loss from somata slightly preceded increases in Fura-6F ratio in this compartment, and this is likely due to leakage of indicator from distal dendrites that experienced the sustained Ca^{2+} response earlier. The degree of indicator loss in TPEN was very similar to that seen in interleaved controls. Fura-6F (360nm) fluorescence measured 5 min after somatic Ca^{2+} deregulation was 14±2% of levels just prior to Ca^{2+} overload in controls vs. 15±2% in TPEN (p=0.64, n=5 each). Under both conditions levels declined to <10% by 10 min after somatic deregulation.

4. Zn^{2+} elevations evaluated with FluoZin-3

The relationship between Zn^{2+} and Ca^{2+} increases was evaluated in neurons co-loaded with FluoZin-3 and Fura-6F. FluoZin-3 fluorescence signals were difficult to detect in dendritic processes (Fig 3A) and therefore the analysis below is restricted to neuronal somata, where reliable measurements could be made. Figure 3B shows a representative example of responses to NMDA. Coincident with the initial Fura-6F spike there was a rapidly increasing FluoZin-3 signal. Unlike the Fura-6F spike, the FluoZin-3 signal did not reset to baseline but remained at an elevated level for the next 25 min. When Fura-6F ratio increases then reported the arrival of sustained Ca^{2+} elevations in the soma, FluoZin-3 levels did not increase, but decreased rapidly. The rate of FluoZin-3 fluorescence loss around this time point was similar to the loss of single wavelength Fura-6F fluorescence (measured at 360nm, Fig 2C), suggesting that the late FluoZin-3 fluorescence decrease was due to loss of indicator from the cell, rather than precipitous decreases in cellular Zn^{2+} levels.

Slice autofluorescence at 490nm is due in part to tissue flavoproteins, and since flavoprotein oxidation state can change in an activity-dependent manner under some conditions (Shibuki et al., 2003; Shuttleworth et al., 2003) autofluorescence changes could potentially complicate analysis of the FluoZin-3 signals. As illustrated in Fig 3, there was no demonstrable autofluorescence change coincident with the initial FluoZin-3 transient, but a slower change was observed that overlapped with the time course of the sustained fluorescence increase after the transient. For this reason, all subsequent FluoZin-3 signals were corrected by subtraction of autofluorescence signals at the same time points, from an adjacent region of stratum pyramidale.

The FluoZin-3 signals from 9 preparations (including the cell from Fig 3) are shown in Fig 4A. Although there was considerable cell-cell variability in the absolute amplitude of responses, all cells showed the same overall pattern; an early FluoZin-3 fluorescence increase followed by variable recovery during a latent period before rapid loss of fluorescence 30-40 min later. The plateau level of FluoZin-3 increase during the latent period (between initial spike and ultimate Ca^{2+} overload) was quite variable (range -8 to 177%, mean 61±20%; n=9). Figure 4B shows the relationship between FluoZin-3 fluorescence loss and arrival of the sustained Ca^{2+} increase and supports the conclusion that FluoZin-3 indicator loss occurs around the time that the Ca^{2+} overload responses arrive.

In a set of slices exposed to TPEN (50μM) FluoZin-3 fluorescence did not increase during NMDA exposure (Fig 4C). When taken together with the insensitivity of FluoZin-3 to Ca^{2+} reported by many groups (see Discussion) this strongly supports the interpretation that FluoZin-3 signals are due to Zn^{2+}, and will be referred to as Zn^{2+} signals in the sections below.

5. Initial transient Zn^{2+} and Fura-6F increases

Figure 4D compares the population averages of the initial Zn^{2+} transient with the initial Fura-6F spike increases for the 9 co-loaded neurons shown in Figure 4A. The records for the different neurons have been aligned with respect to the peak of Fura-6F spike, and show that peak of the Zn^{2+} and Fura-6F increases are coincident, but the Zn^{2+} transient is considerably broader. It is possible that the rise times of Ca^{2+} and Zn^{2+} increases are actually very similar, since the low affinity Fura-6F makes Ca^{2+} increases below about 500nM undetectable. These initial smaller changes have been measured using Fura-2 and occupy a period of 2-3 min (Fig 2A Vander Jagt et al., 2008). However it is also possible that Zn^{2+} increases precede and outlast Ca^{2+} increases, and the full relationship between the two signals may require development of high affinity Ca^{2+} indicators that retain apparent insensitivity to Zn^{2+} when tested in neurons. The same considerations apply to the apparently slower and less complete recovery of FluoZin-3 responses after the initial peak responses.

6. Extracellular Zn^{2+} chelation using Ca-EDTA

To assess the source(s) of Zn^{2+} responsible for FluoZin-3 signals, we examined the effects of selective chelation of Zn^{2+} in the extracellular space, by using Ca-EDTA. Ca-EDTA has high affinity for Zn^{2+} ($K_D=8\times10^{-14}$M) (Lee et al., 2002), but unlike TPEN is not membrane permeable. Extended exposures to Ca-EDTA alone (up to 30 min, n=3) did not modify initial FluoZin-3 fluorescence levels (data not shown). This suggests that there is not substantial depletion of cytosolic Zn^{2+} as a result of extracellular chelation, in contrast to the described loss of fluorescence attributed to Zn^{2+} in synaptic vesicles by similar procedures (Frederickson et al., 2002). Figure 5A shows that (unlike TPEN) Ca-EDTA (1 mM) did not block initial intracellular Zn^{2+} increases during NMDA. Peak Zn^{2+} increases were of very similar amplitude (281±30%) and latency (6.4±1.1min, n=5) to those observed in control cells (Figure 4). Taken together with TPEN data, these results suggest that the source(s) of Zn^{2+} responsible for initial transients may be due to liberation from intracellular binding proteins. An alternative

possibility is that Zn^{2+} may enter from the extracellular space from release sites very close to Zn^{2+} entry routes, since the relatively slow binding kinetics of Ca-EDTA (Kay, 2003) may not be sufficient rapid to chelate Zn^{2+} before neuronal entry (as considered in Dietz et al., 2008)).

The recovery of FluoZin-3 fluorescence after initial transients was more complete in Ca-EDTA than under control conditions. Thus there was recovery to 7±29% by 15 min after the spike, compared to the larger (but variable) plateau levels observed in control conditions. This raises the possibility that sustained influx of Zn^{2+} from the extracellular space may contribute to the plateau responses in many cells. Ca-EDTA did not significantly reduce initial Fura-6F spikes (19.4±3.6 vs. 15.8±3.4μM, control and Ca-EDTA respectively; p=0.5, n=6 each). Likewise, the arrival of Ca^{2+} overload responses at somata was not significantly delayed (40.6±3.1 vs. 48.4±5.0 min, control and Ca-EDTA respectively, p=0.2, n=6 each).

8. Effects of Ca^{2+} removal on intracellular Zn^{2+} increases

We addressed the question of whether Zn^{2+} increases might be dependent on cytosolic Ca^{2+} accumulation. Extracellular Ca^{2+} was washed out (without addition of any chelators) 10 min prior to onset of NMDA exposure, and 2mM Ca^{2+} was not re-introduced until after initial spike responses should have been completed (i.e. 15 min after addition of NMDA). From measurements of Ca^{2+} in the recording chamber, full restoration of extracellular [Ca^{2+}] required an additional ~2 min.

Figure 6 shows that reducing Ca^{2+} influx during the initial period reduced, but did not prevent intracellular Zn^{2+} increases. Initial transient FluoZin-3 increases reached 47.3±11.8 % (n=6), a substantially lower level than in control conditions (compare with Figs. 4A&5A). FluoZin-3 fluorescence then returned to near-baseline levels until reestablishment of 2mM extracellular Ca^{2+}, when Zn^{2+} levels promptly increased to a new plateau level (mean 55.0±12.2% n=6). The plots in Figure 6A are aligned (upper panel: FluoZin-3, lower panel: Fura-6F) so that it can be seen that FluoZin-3 signals dropped sharply as sustained Ca^{2+} increases arrived at the soma. Figure 6A (lower panel) also shows a small residual increase in Fura-6F signal prior to re-introduction of Ca^{2+} (at t~15 min), possibly the result of enhanced interaction of Zn^{2+} with Fura-6F in Ca^{2+}-free conditions (see (Devinney et al., 2005)).

Discussion

1. General

We draw three main conclusions from these results. Firstly, Zn^{2+} binding to Fura-6F does not appear responsible for previously-reported sustained Ca^{2+} increases, that originate in distal locations in apical dendrites and then propagate to somata. These dendritic signals appear to be due to excessive Ca^{2+} influx and accumulation, ultimately leading to Ca^{2+} overload in somata and causing acute injury to these neurons (Vander Jagt et al., 2008). Secondly, sustained NMDA exposure leads to significant increases in neuronal Zn^{2+} accumulation that are detectable using single neurons loaded with FluoZin-3. Zn^{2+} increases derive from endogenous sources within the slice, and are chelatable by TPEN but are largely unaffected by the slow membrane-impermeant chelator Ca-EDTA. Thirdly, Zn^{2+} increases appear to contribute to the progression of degenerative Ca^{2+} signals along apical dendrites, and we speculate that detrimental effects of Zn^{2+} accumulation leads to progressive metabolic dysfunction, ultimately contributing to regional loss of Ca^{2+} homeostasis.

2. Potential interference of Zn^{2+} with Fura-6F signals

A high-affinity interaction of Zn^{2+} with the widely-utilized Ca^{2+}-indicator Fura-2 has been noted for more than 2 decades (Grynkiewicz et al., 1985; Cheng and Reynolds, 1998) and the high sensitivity of related Ca^{2+} indicators to Zn^{2+} has been reported in subsequent studies in

free solution (Simons, 1993; Atar et al., 1995; Sensi et al., 1997; e.g. Hyrc et al., 2000; Devinney et al., 2005). However when these indicators are loaded into neurons at concentrations suitable for live cell imaging, the sensitivity to Zn^{2+} appears to decrease substantially. An important contributor to this effect is likely to be the relatively high indicator concentrations that are usually required for cellular studies, since as indicator concentration exceeds K_D, the former makes progressively larger contributions to binding, and large differences in affinity become less meaningful (Dineley et al., 2002). When recordings are then made with physiological Ca^{2+} concentrations, the contribution of Zn^{2+} binding to the total indicator signal is small (Devinney et al., 2005). It is also possible that a range of intracellular constituents could also contribute to diminishing apparent Zn^{2+} sensitivity within cells (Marchi et al., 2000), although the impact of such interactions in neuronal recordings has been questioned (Devinney et al., 2005). These observations are important, since they emphasize that the Zn^{2+} and Ca^{2+} signals can be distinguished within neurons with existing fluorescent indicators, despite concerns raised from affinity studies in free solution (Martin et al., 2006). In a recent study of CA1 neurons co-loaded with Fura-6F and FluoZin-3, we detected Zn^{2+} increases during ouabain exposures without demonstrable increases in Fura-2 or Fura-6F, clearly showing that Zn^{2+} did not meaningfully interact with Fura-type indicators under those conditions (Dietz et al., 2008). However the present study is a little different, because NMDA produced an initial transient increase in both Fura-6F and FluoZin-3 signals, and selective intracellular chelation of Zn^{2+} significantly reduced the amplitude of Fura-6F spikes (see Fig 2A). Thus the potential contributions of Zn^{2+} to initial Fura-6F spikes needs to be considered (see below). In contrast to the initial Fura-6F spikes, it is important to emphasize that the sustained Fura-6F increases that propagate along dendritic processes can not be explained by Zn^{2+} accumulation, since they were only slowed but otherwise unaffected by TPEN and prevented by Ca^{2+} removal. The Ca^{2+} levels achieved during the overload response readily saturated the low affinity indicator used, and because of this it is not yet known whether TPEN may have some effect on the final Ca^{2+} concentrations that are achieved. However, it is likely rapid membrane compromise results in very high intracellular Ca^{2+} levels during this phase of the response, and that Ca^{2+} overload remains the logical explanation for these propagating Fura-6F signals associated with degeneration.

3. The early Fura-6F spike

We previously showed that initial Fura-6F spike responses were almost abolished by nominally Ca^{2+}-free media (Vander Jagt et al., 2008) and see also Figure 6), however from this result alone it can not be concluded that Ca^{2+} is solely responsible for these transients. For example, it has been suggested that un-avoidable contamination of Ca^{2+} stock solutions with Zn^{2+} could make significant contributions to indicator signals (Kay, 2004) and it is thus possible that removal of Ca^{2+} from the media also removes an amount of Zn^{2+} (Dineley, 2007). This does not appear to be the case here, since the chelator Ca-EDTA (1mM) should remove contaminating Zn^{2+} from the ACSF, and did not reduce any component of Fura-6F signals.

Although Zn^{2+} binding to Fura-6F will be limited by the factors described above, Zn^{2+} may still bind to Fura-6F during initial spikes, but we note that this would not necessarily be expected to contribute to increases in Fura-6F ratio. The spectra produced by Ca^{2+} and Zn^{2+} binding to Fura indicators are slightly shifted relative to each other, so that the 380nm fluorescence changes are significantly less with Zn^{2+} than with Ca^{2+}. This has the consequence of actually decreasing cumulative Fura ratio changes, when measurements are made in the presence of Ca^{2+} (Devinney et al., 2005). Under the conditions of our experiments, we would therefore predict that TPEN should produce an increase in Fura-6F ratio during the initial spike response, if Zn^{2+} binding to Fura-6F were significant during this event. In fact the converse was observed, suggesting that a stronger effect is that Zn^{2+} elevations somehow contribute to mechanisms underlying Ca^{2+} increases.

4. FluoZin-3 signals

In contrast to potential concerns about Zn^{2+} binding to Fura-indicators, the converse situation appears more simple, since a number of groups have reported that Ca^{2+} binding to FluoZin-3 is negligible, even with very high Ca^{2+} concentrations (Gee et al., 2002; Kay, 2004; Devinney et al., 2005). A recent report has questioned this conclusion (Martin et al., 2006) and possible reasons for the discrepancy in this report have been debated (Dineley, 2007). The present work supports a lack of Ca^{2+}-sensitivity of FluoZin-3. Selective chelation of Zn^{2+} with TPEN completely abolished initial FluoZin-3 signals, despite the fact that large Ca^{2+} elevations (~5μM) were still occurring and were readily detected with Fura-6F. Thus it appears that significant amounts of Zn^{2+} are mobilized together with Ca^{2+} during early transient responses.

Figure 4 demonstrates that Zn^{2+} levels remain above baseline in many neurons during the latent period before arrival of Ca^{2+} overload responses at the soma. These sustained elevations are probably not related to subsequent Ca^{2+} overload responses, since Ca-EDTA prevented the sustained Zn^{2+} elevations but did not have a significant effect on the timing of degenerative Ca^{2+} signals. This suggests that the early transient responses may be more important in degeneration.

After irrecoverable Ca^{2+} overload responses are established, neurons leak charged indicators and fluorescence is lost from the cell. This has been described previously for Ca^{2+} indicators, where sustained ratio increases (indicating persistently high Ca^{2+} levels) are observed in the face of loss of indicator fluorescence levels (Randall and Thayer, 1992; Shuttleworth and Connor, 2001; Avignone et al., 2005; Vander Jagt et al., 2008). A similar loss of FluoZin-3 fluorescence was observed in the present study, where FluoZin-3 signals in somata promptly decreased as the Ca^{2+} overload response approached the region (Figures 3 & 6). This loss of indicator fluorescence makes it difficult to determine whether Zn^{2+} levels actually increase first during the period of severe Ca^{2+} overload, or whether Zn^{2+} elevations may occur after this time point as a consequence of Ca^{2+} toxicity. The development of ratiometric indicators for Zn^{2+} with appropriate sensitivity and selectivity to address this question would be helpful for future studies.

5. Contribution of Zn^{2+} to the mechanism(s) of degenerative signaling along dendrites

Prevention of intracellular Zn^{2+} accumulation with TPEN produced a relatively small, but significant delay in the arrival of dendritic Ca^{2+} increases at somata (Fig. 2), suggesting that intracellular Zn^{2+} increases do influence the initiation and/or propagation of mechanisms responsible for Ca^{2+} deregulation along the dendrite.

Zn^{2+} is known to inhibit NMDA receptors (Peters et al., 1987; Westbrook and Mayer, 1987). However, this can not explain the longer delay in Ca^{2+} overload response with TPEN, since an increase in NMDA activation and accelerated injury should result if this were the dominant effect of Zn^{2+} in these experiments. Zn^{2+}-dependent inhibition of metabolism is a likely mechanism participating in the origin of the injurious Ca^{2+} overload seen here. We recently showed that the progression of Ca^{2+} overload along dendrites was not due to a “feed-forward” Ca^{2+}-dependent mechanism, whereby excessive Ca^{2+} loading was initially responsible for causing deregulation of adjacent segments of dendrite. Instead, the metabolic consequences of excessive Na^{+} loading during extended NMDA exposures appeared to be a more likely candidate, with Ca^{2+} overload following, presumably after ATP supply in a region of dendrite became irrecoverably lost (Vander Jagt et al., 2008b). Zn^{2+} has been shown to inhibit mitochondrial function (Skulachev et al., 1967; Sensi et al., 2003; Gazaryan et al., 2007) and also impair glycolysis by inhibition of glyceraldyhyde-3 phosphate dehydrogenase (Sheline et al., 2000). Zn^{2+} could also contribute to Ca^{2+} overload by blocking Na^{+}/K^{+} ATPase activity (Donaldson et al., 1971; Manzerra et al., 2001) and thereby contributing to excessive

accumulation of intracellular Na^+ and reversal of sodium-calcium exchangers. However, we have found that sodium-calcium exchange reversal does not appear to be a major Ca^{2+} influx pathway in this model of NMDA exposure (Dietz et al., 2007). As noted above, even with chelation of Zn^{2+}, the responses are merely delayed and were not abolished. Thus any deleterious effects of Zn^{2+} impairing ATP re-supply are likely to be additive with Zn^{2+}-independent mechanisms of ATP depletion, including persistent Na^+-dependent activation of Na^+/K^+/ATPase activity.

6. Sources of Zn^{2+}

As noted in the Introduction, mobilization of Zn^{2+} from presynaptic sources, and/or liberation from intracellular binding proteins are two major sources of endogenous Zn^{2+} that can be considered for the Zn^{2+} increases described here. Zn^{2+} accumulates in synaptic vesicles following accumulation through ZnT3 transporters (Palmiter et al., 1996), and can be liberated following synaptic stimulation in the hippocampus (Assaf and Chung, 1984; Howell et al., 1984; Qian and Noebels, 2006). It is possible that NMDA releases Zn^{2+} from synaptic vesicles in the CA1 region, and Zn^{2+} then is taken up by CA1 neurons. The fact that the extracellular Zn^{2+} chelator (Ca-EDTA) did not prevent Zn^{2+} increases tends to argue against this possibility, however it is possible that the kinetics of Ca-EDTA are too slow to prevent effective sequestration, if the synaptic release sites were very close to postsynaptic influx routes. Such a scenario was proposed recently to explain the lack of effect of Ca-EDTA on Zn^{2+} increases that were deduced to be due to influx from the extracellular space (Dietz et al., 2008). If synaptic release and influx were involved and followed by intracellular transport to the soma, then a reduction in Ca^{2+}-dependent vesicle fusion during NMDA exposure could explain the inhibitory effect of Ca^{2+} removal on the amplitude of measured Zn^{2+} increases. We also note that a number of factors influence the availability of synaptically-released Zn^{2+} and it is quite possible that synaptic contributions to initial Zn^{2+} increases may be larger in preparations from older animals, or when recording temperatures are increased (Frederickson et al., 2006).

An alternative possibility is that the source of free intracellular Zn^{2+} in these studies may be predominantly from intracellular binding proteins. Neurons have relatively large stores of Zn^{2+} that are normally associated with binding proteins such as Metallothionein III. This Zn^{2+} can be readily mobilized by excitotoxic or oxidative insults (Aizenman et al., 2000; Lee et al., 2003; Sensi et al., 2003; Bossy-Wetzel et al., 2004). Micromolar Ca^{2+} increases could cause liberation of Zn^{2+} from intracellular binding sites and (together with synaptic effects discussed above) could contribute to the partial Ca^{2+}-dependence of Zn^{2+} increases observed in the present work. Zn^{2+} release from metallothioneins could be triggered by reactive oxygen species generated in a Ca^{2+}-dependent manner by mitochondria, nitric oxide synthase or phospholipase C (Frederickson et al., 2004; Dineley et al., 2008). In addition, Ca^{2+}-dependent acidification caused by NMDA receptor activation could play a significant role, since intracellular pH decreases are well-established to mobilize Zn^{2+} from intracellular stores (Jiang et al., 2000; Frazzini et al., 2007).

7. Conclusion

Simultaneous imaging of changes in intracellular Ca^{2+} and Zn^{2+} in single CA1 neurons, using Fura-6F and FlouZin-3, revealed significant accumulation of both Zn^{2+} and Ca^{2+} during extended NMDA exposures. Excessive somatic Ca^{2+} accumulation (following apical dendrite Ca^{2+} deregulation) appeared to be ultimately responsible for neuronal injury, but Zn^{2+} increases may contribute to initiation and progression of degenerative Ca^{2+} signaling.

Acknowledgements

Supported by NIH grants NS051288 (C.W.S.) and NS36548 (J.H.W.).

References

Aizenman E, Stout AK, Hartnett KA, Dineley KE, McLaughlin B, Reynolds IJ. Induction of neuronal apoptosis by thiol oxidation: putative role of intracellular zinc release. J Neurochem 2000;75:1878–1888. [PubMed: 11032877]

Arslan P, Di Virgilio F, Beltrame M, Tsien RY, Pozzan T. Cytosolic Ca2+ homeostasis in Ehrlich and Yoshida carcinomas. A new, membrane-permeant chelator of heavy metals reveals that these ascites tumor cell lines have normal cytosolic free Ca2+ J Biol Chem 1985;260:2719–2727. [PubMed: 3919006]

Arundine M, Tymianski M. Molecular mechanisms of calcium-dependent neurodegeneration in excitotoxicity. Cell Calcium 2003;34:325–337. [PubMed: 12909079]

Assaf SY, Chung SH. Release of endogenous Zn2+ from brain tissue during activity. Nature 1984;308:734–736. [PubMed: 6717566]

Atar D, Backx PH, Appel MM, Gao WD, Marban E. Excitation-transcription coupling mediated by zinc influx through voltage-dependent calcium channels. J Biol Chem 1995;270:2473–2477. [PubMed: 7852308]

Avignone E, Frenguelli BG, Irving AJ. Differential responses to NMDA receptor activation in rat hippocampal interneurons and pyramidal cells may underlie enhanced pyramidal cell vulnerability. Eur J Neurosci 2005;22:3077–3090. [PubMed: 16367774]

Bossy-Wetzel E, Talantova MV, Lee WD, Scholzke MN, Harrop A, Mathews E, Gotz T, Han J, Ellisman MH, Perkins GA, Lipton SA. Crosstalk between nitric oxide and zinc pathways to neuronal cell death involving mitochondrial dysfunction and p38-activated K+ channels. Neuron 2004;41:351–365. [PubMed: 14766175]

Cheng C, Reynolds IJ. Calcium-sensitive fluorescent dyes can report increases in intracellular free zinc concentration in cultured forebrain neurons. J Neurochem 1998;71:2401–2410. [PubMed: 9832138]

Choi DW. Calcium-mediated neurotoxicity: relationship to specific channel types and role in ischemic damage. Trends Neurosci 1988;11:465–469. [PubMed: 2469166]

Choi DW, Koh JY. Zinc and brain injury. Annu Rev Neurosci 1998;21:347–375. [PubMed: 9530500]

Christine CW, Choi DW. Effect of zinc on NMDA receptor-mediated channel currents in cortical neurons. J Neurosci 1990;10:108–116. [PubMed: 1688929]

Connor, JA.; Shuttleworth, CW. Intracellular Ca2+ signals underlying rapid and delayed neuronal death in mature CNS neurons. In: Lin, RCS., editor. New concepts in cerebral ischemia. CRC Press; 2001. p. 113-134.

Devinney MJ 2nd, Reynolds IJ, Dineley KE. Simultaneous detection of intracellular free calcium and zinc using fura-2FF and FluoZin-3. Cell Calcium 2005;37:225–232. [PubMed: 15670869]

Dietz RM, Kiedrowski L, Shuttleworth CW. Contribution of Na(+)/Ca(2+) exchange to excessive Ca(2+) loading in dendrites and somata of CA1 neurons in acute slice. Hippocampus 2007;17:1049–1059. [PubMed: 17598158]

Dietz RM, Weiss JH, Shuttleworth CW. Zn2+ influx is critical for some forms of spreading depression in brain slices. J Neurosci 2008;28:8014–8024. [PubMed: 18685026]

Dineley KE. On the use of fluorescent probes to distinguish Ca2+ from Zn2+ in models of excitotoxicity. Cell Calcium 2007;42:341–342. [PubMed: 17343910]author reply 343-344

Dineley KE, Malaiyandi LM, Reynolds IJ. A reevaluation of neuronal zinc measurements: artifacts associated with high intracellular dye concentration. Mol Pharmacol 2002;62:618–627. [PubMed: 12181438]

Dineley KE, Devinney MJ 2nd, Zeak JA, Rintoul GL, Reynolds IJ. Glutamate mobilizes [Zn2+] through Ca2+ -dependent reactive oxygen species accumulation. J Neurochem 2008;106:2184–2193. [PubMed: 18624907]

Donaldson J, St Pierre T, Minnich J, Barbeau A. Seizures in rats associated with divalent cation inhibition of NA + -K + -ATP'ase. Can J Biochem 1971;49:1217–1224. [PubMed: 4257414]

Frazzini V, Rapposelli IG, Corona C, Rockabrand E, Canzoniero LM, Sensi SL. Mild Acidosis Enhances Ampa Receptor-Mediated Intracellular Zinc Mobilization in Cortical Neurons. Mol Med. 2007

Frederickson CJ, Maret W, Cuajungco MP. Zinc and excitotoxic brain injury: a new model. Neuroscientist 2004;10:18–25. [PubMed: 14987444]

Frederickson CJ, Koh JY, Bush AI. The neurobiology of zinc in health and disease. Nat Rev Neurosci 2005;6:449–462. [PubMed: 15891778]

Frederickson CJ, Suh SW, Koh JY, Cha YK, Thompson RB, LaBuda CJ, Balaji RV, Cuajungco MP. Depletion of intracellular zinc from neurons by use of an extracellular chelator in vivo and in vitro. J Histochem Cytochem 2002;50:1659–1662. [PubMed: 12486088]

Frederickson CJ, Giblin LJ 3rd, Balaji RV, Masalha R, Frederickson CJ, Zeng Y, Lopez EV, Koh JY, Chorin U, Besser L, Hershfinkel M, Li Y, Thompson RB, Krezel A. Synaptic release of zinc from brain slices: factors governing release, imaging, and accurate calculation of concentration. J Neurosci Methods 2006;154:19–29. [PubMed: 16460810]

Gazaryan IG, Krasinskaya IP, Kristal BS, Brown AM. Zinc irreversibly damages major enzymes of energy production and antioxidant defense prior to mitochondrial permeability transition. J Biol Chem 2007;282:24373–24380. [PubMed: 17565998]

Gee KR, Zhou ZL, Ton-That D, Sensi SL, Weiss JH. Measuring zinc in living cells. A new generation of sensitive and selective fluorescent probes. Cell Calcium 2002;31:245–251. [PubMed: 12098227]

Grynkiewicz G, Poenie M, Tsien RY. A new generation of Ca2+ indicators with greatly improved fluorescence properties. J Biol Chem 1985;260:3440–3450. [PubMed: 3838314]

Hechtenberg S, Beyersmann D. Differential control of free calcium and free zinc levels in isolated bovine liver nuclei. Biochem J 1993;289(Pt 3):757–760. [PubMed: 8382049]

Howell GA, Welch MG, Frederickson CJ. Stimulation-induced uptake and release of zinc in hippocampal slices. Nature 1984;308:736–738. [PubMed: 6717567]

Hyrc KL, Bownik JM, Goldberg MP. Ionic selectivity of low-affinity ratiometric calcium indicators: mag-Fura-2, Fura-2FF and BTC. Cell Calcium 2000;27:75–86. [PubMed: 10756974]

Jiang LJ, Vasak M, Vallee BL, Maret W. Zinc transfer potentials of the alpha - and beta-clusters of metallothionein are affected by domain interactions in the whole molecule. Proc Natl Acad Sci U S A 2000;97:2503–2508. [PubMed: 10716985]

Kay AR. Evidence for chelatable zinc in the extracellular space of the hippocampus, but little evidence for synaptic release of Zn. J Neurosci 2003;23:6847–6855. [PubMed: 12890779]

Kay AR. Detecting and minimizing zinc contamination in physiological solutions. BMC Physiol 2004;4:4. [PubMed: 15113426]

Lee JM, Zipfel GJ, Park KH, He YY, Hsu CY, Choi DW. Zinc translocation accelerates infarction after mild transient focal ischemia. Neuroscience 2002;115:871–878. [PubMed: 12435425]

Lee JY, Kim JH, Palmiter RD, Koh JY. Zinc released from metallothionein-iii may contribute to hippocampal CA1 and thalamic neuronal death following acute brain injury. Exp Neurol 2003;184:337–347. [PubMed: 14637104]

Manzerra P, Behrens MM, Canzoniero LM, Wang XQ, Heidinger V, Ichinose T, Yu SP, Choi DW. Zinc induces a Src family kinase-mediated up-regulation of NMDA receptor activity and excitotoxicity. Proc Natl Acad Sci U S A 2001;98:11055–11061. [PubMed: 11572968]

Marchi B, Burlando B, Panfoli I, Viarengo A. Interference of heavy metal cations with fluorescent Ca2 + probes does not affect Ca2+ measurements in living cells. Cell Calcium 2000;28:225–231. [PubMed: 11032778]

Martin JL, Stork CJ, Li YV. Determining zinc with commonly used calcium and zinc fluorescent indicators, a question on calcium signals. Cell Calcium 2006;40:393–402. [PubMed: 16764924]

Nicholls DG, Budd SL. Mitochondria and neuronal survival. Physiol Rev 2000;80:315–360. [PubMed: 10617771]

Palmiter RD, Cole TB, Quaife CJ, Findley SD. ZnT-3, a putative transporter of zinc into synaptic vesicles. Proc Natl Acad Sci U S A 1996;93:14934–14939. [PubMed: 8962159]

Peters S, Koh J, Choi DW. Zinc selectively blocks the action of N-methyl-D-aspartate on cortical neurons. Science 1987;236:589–593. [PubMed: 2883728]

Qian J, Noebels JL. Exocytosis of vesicular zinc reveals persistent depression of neurotransmitter release during metabotropic glutamate receptor long-term depression at the hippocampal CA3-CA1 synapse. J Neurosci 2006;26:6089–6095. [PubMed: 16738253]

Randall RD, Thayer SA. Glutamate-induced calcium transient triggers delayed calcium overload and neurotoxicity in rat hippocampal neurons. J Neurosci 1992;12:1882–1895. [PubMed: 1349638]

Sensi SL, Canzoniero LM, Yu SP, Ying HS, Koh JY, Kerchner GA, Choi DW. Measurement of intracellular free zinc in living cortical neurons: routes of entry. J Neurosci 1997;17:9554–9564. [PubMed: 9391010]

Sensi SL, Ton-That D, Sullivan PG, Jonas EA, Gee KR, Kaczmarek LK, Weiss JH. Modulation of mitochondrial function by endogenous Zn2+ pools. Proc Natl Acad Sci U S A 2003;100:6157–6162. [PubMed: 12724524]

Sheline CT, Behrens MM, Choi DW. Zinc-induced cortical neuronal death: contribution of energy failure attributable to loss of NAD(+) and inhibition of glycolysis. J Neurosci 2000;20:3139–3146. [PubMed: 10777777]

Shibuki K, Hishida R, Murakami H, Kudoh M, Kawaguchi T, Watanabe M, Watanabe S, Kouuchi T, Tanaka R. Dynamic imaging of somatosensory cortical activity in the rat visualized by flavoprotein autofluorescence. J Physiol 2003;549:919–927. [PubMed: 12730344]

Shuttleworth CW, Connor JA. Strain-dependent differences in calcium signaling predict excitotoxicity in murine hippocampal neurons. J Neurosci 2001;21:4225–4236. [PubMed: 11404408]

Shuttleworth CW, Brennan AM, Connor JA. NAD(P)H fluorescence imaging of postsynaptic neuronal activation in murine hippocampal slices. J Neurosci 2003;23:3196–3208. [PubMed: 12716927]

Simons TJ. Measurement of free Zn2+ ion concentration with the fluorescent probe mag-fura-2 (furaptra). J Biochem Biophys Methods 1993;27:25–37. [PubMed: 8409208]

Skulachev VP, Chistyakov VV, Jasaitis AA, Smirnova EG. Inhibition of the respiratory chain by zinc ions. Biochem Biophys Res Commun 1967;26:1–6. [PubMed: 4291553]

Vander Jagt, TA.; Weiss, JH.; Shuttleworth, CW. Contribution of intracellular Zn2+ to progressive loss of Ca+ homeostasis in CA1 neurons in hippocampal slices. 2007 Meeting Planner Society for Neuroscience; 2007; 2007. Online 55.5

Vander Jagt TA, Connor JA, Shuttleworth CW. Localized loss of Ca2+ homeostasis in neuronal dendrites is a downstream consequence of metabolic compromise during extended NMDA exposures. J Neurosci 2008;28:5029–5039. [PubMed: 18463256]

Weiss JH, Sensi SL, Koh JY. Zn(2+): a novel ionic mediator of neural injury in brain disease. Trends Pharmacol Sci 2000;21:395–401. [PubMed: 11050320]

Weiss JH, Hartley DM, Koh JY, Choi DW. AMPA receptor activation potentiates zinc neurotoxicity. Neuron 1993;10:43–49. [PubMed: 7678965]

Westbrook GL, Mayer ML. Micromolar concentrations of Zn2+ antagonize NMDA and GABA responses of hippocampal neurons. Nature 1987;328:640–643. [PubMed: 3039375]

Abbreviations

ACSF
: artificial cerebrospinal fluid

DMSO
: Dimethyl sulfoxide

EDTA
: Ethylenediaminetetraacetate

NMDA
: N-Methyl-D-aspartic acid

TPEN
: N,N,N′,N′-Tetrakis(2-pyridylmethyl) ethylenediamine

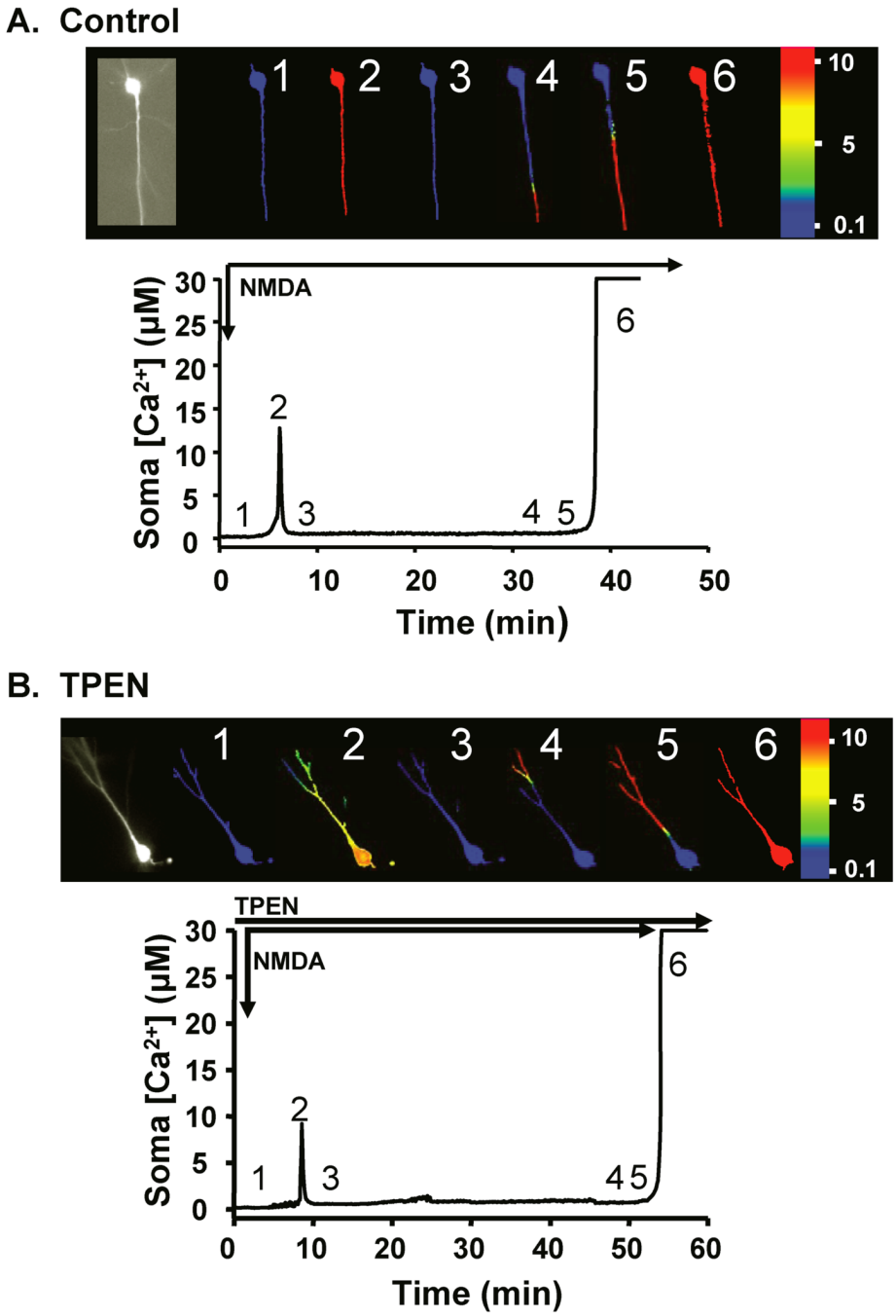

Figure 1. TPEN did not prevent progressive Ca^{2+} overload

A: Fura-6F responses in a CA1 neuron during NMDA exposure (5μM). Left panel; 380nm excitation image of filled neuron. Subsequent panels are pseudo-color images, masked and calibrated to estimated Ca^{2+} levels before (1) and during NMDA exposure (2-6). An initial Ca^{2+} spike (2) was followed by recovery to near basal levels (3) throughout the neuron. After a significant delay, sustained Ca^{2+} increases appeared in distal dendrite locations (4-5) and slowly propagated into the soma (6). Plot shows data extracted from a region of interest in the soma. **B:** As in "A," except that the slice was pre-exposed to the Zn^{2+} chelator TPEN (50μM). The general characteristics of the Fura-6F response appeared very similar, with an initial

transient increase, recovery and long delay before progression of sustained Ca^{2+} increase from apical dendrite into the soma.

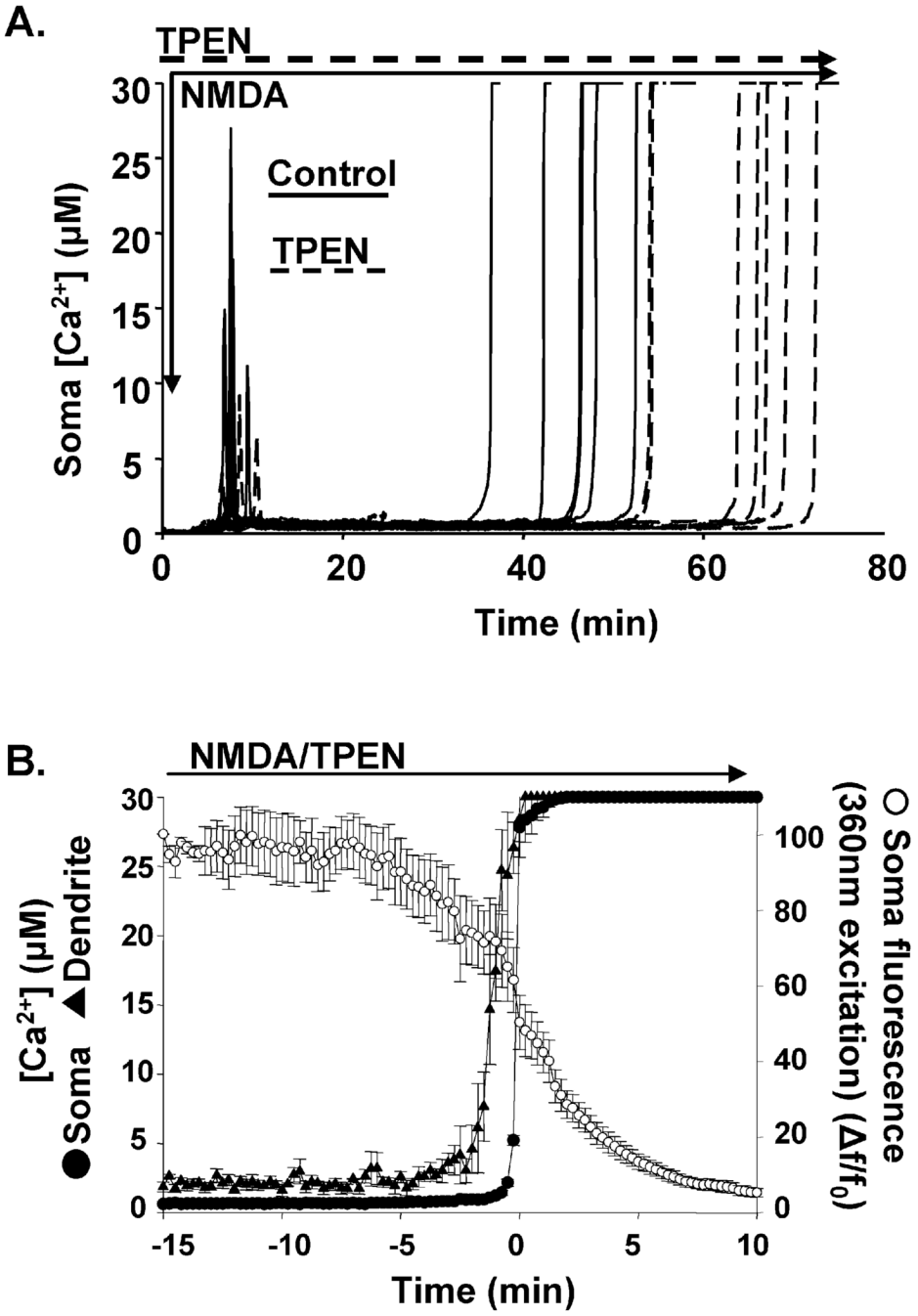

Figure 2. TPEN delayed the arrival of sustained dendritic Ca^{2+} increases at the soma

A: Each trace represents the Fura-6F response recorded from the soma of a single neuron, calibrated to estimated Ca^{2+} levels. Studies in a set of control slices (*solid lines*) were interleaved with slices slices pre-exposed to TPEN (50μM; *dashed lines*). TPEN significantly delayed the arrival of sustained Ca^{2+} increases at somata ($p<0.01$ n=7 each). **B:** TPEN did not prevent rapid neuronal injury after establishment of Ca^{2+} overload in somata. The rising phases of sustained Ca^{2+} increases in somata were aligned (time 0; filled *circles*, n=5) and the preceding responses from a region of apical proximal dendrite (40-60 μm from somata; *triangles*) are also included for 3 neurons where dendrites were sufficiently within the plane of focus. Fluorescence intensity at the isobestic point for Fura-6F (360nm; *open circles*) was

monitored to determine indicator loss, and despite the presence of TPEN, showed dramatic loss as sustained Ca^{2+} levels became established in somata.

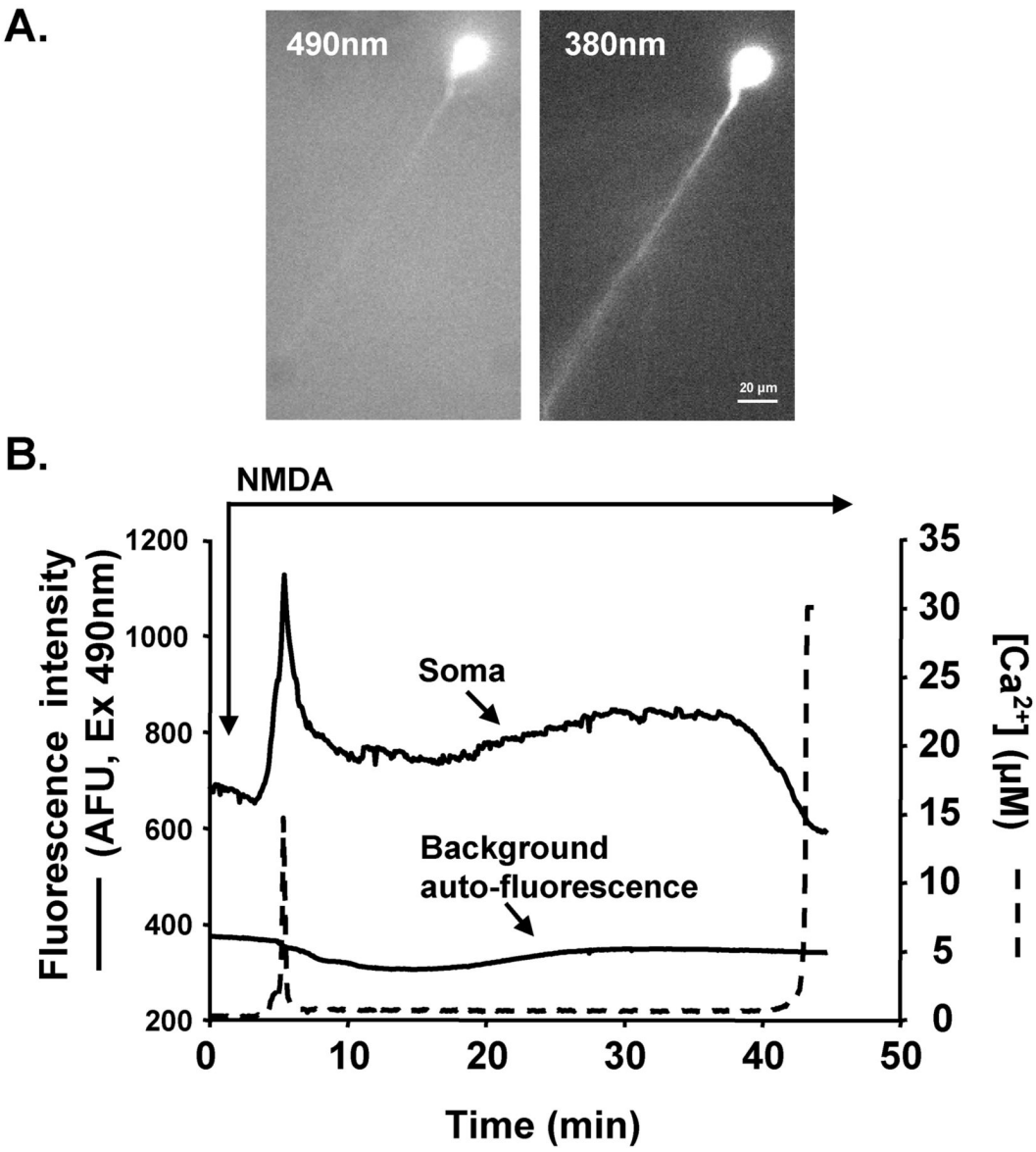

Figure 3. Intracellular Zn^{2+} increases during NMDA exposure

A: Fluorescence images of a single CA1 neuron co-loaded with FluoZin-3 (490nm) and Fura-6F (360nm). **B:** Data extracted from the soma of the neuron shown in A, during NMDA exposure. An initial FluoZin-3 increase (*solid line, top trace*) was observed soon after NMDA addition, coincident with the early spike in the Fura-6F signal (*dashed line*). After a partial recovery, Fluozin-3 fluorescence remained elevated during the latent period, and then decreased to below baseline levels when the sustained Ca^{2+} response arrived at the soma. Autofluorescence (490nm) from a region of stratum pyramidale outside the neuron (*solid line, bottom trace*) showed no initial transient, but a slow fluctuation during the latent period.

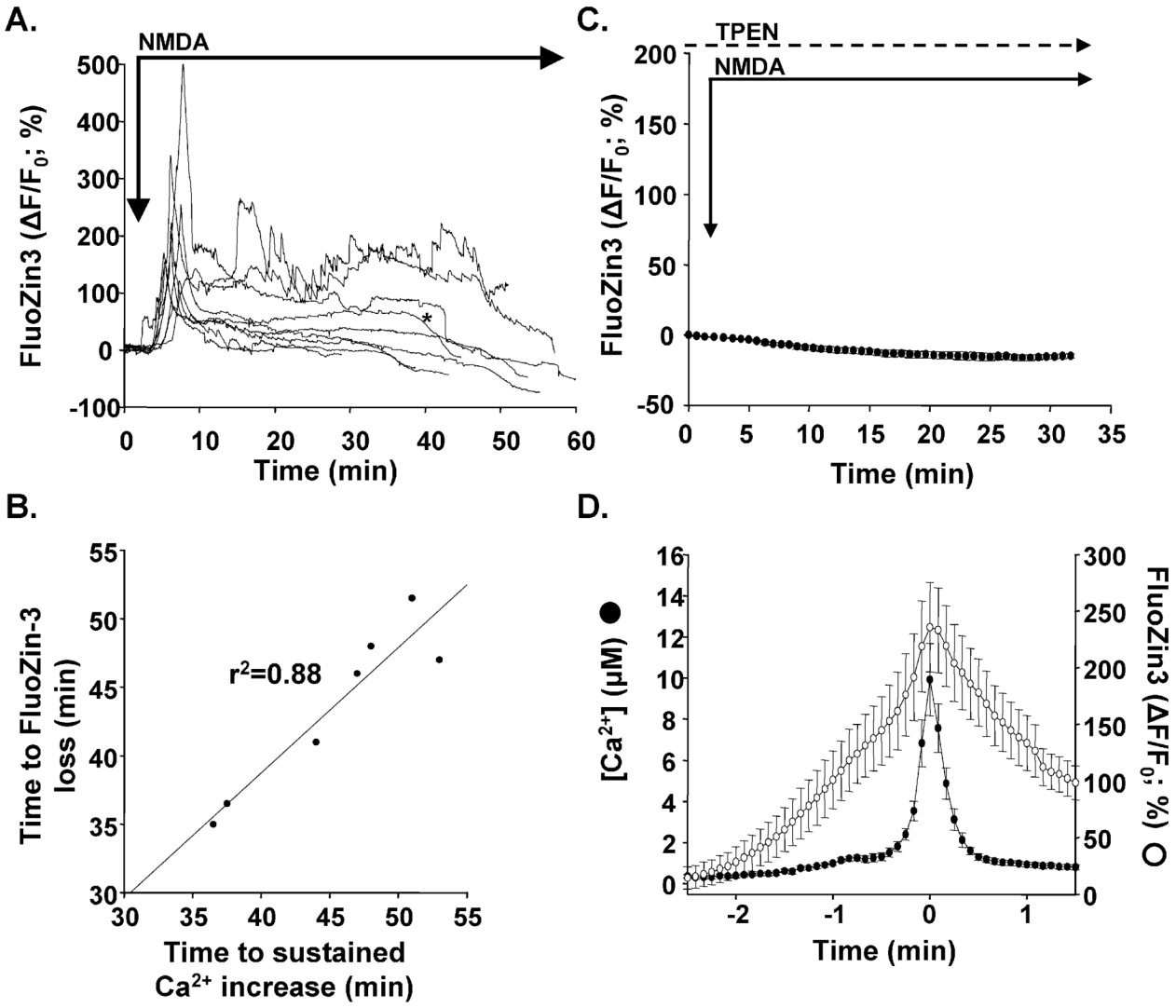

Figure 4. Characteristics of Zn^{2+} increases

A: FluoZin-3 responses during NMDA exposure from 9 preparations, corrected for slow autofluorescence changes. All show initial transient FluoZin-3 increases, which then recover to variable degrees for ~30 min before fluorescence levels decline sharply. **B:** Late FluoZin-3 signal loss correlated strongly with sustained Ca^{2+} increases in somata. Clear increases in the rate of FluoZin-3 fluorescence loss was detectable in 7/9 neurons. For these neurons, the time at which 50% FluoZin-3 fluorescence intensity (compared with plateau levels prior to arrival of Ca^{2+} overload) is lost is plotted against the time of half-maximal Ca^{2+} increase as the sustained Ca^{2+} response invaded somata. **C:** TPEN prevented FluoZin-3 fluorescence increases. TPEN (50μM) was added 20 min prior to NMDA and remained throughout the experiment. No initial or delayed fluorescence increases were observed during NMDA (mean ±SEM, n=4). **D:** Initial transient FluoZin-3 increases from the responses illustrated in A are shown at an expanded time base (*open circles*), together with initial Fura-6F transients from the same neurons (*filled circles*). Records were aligned with the timing of the peak Fura-6F response in each cell (n=9) and show that both signals peaked at the same time, although the duration of the Fura-6F transients appears significantly shorter.

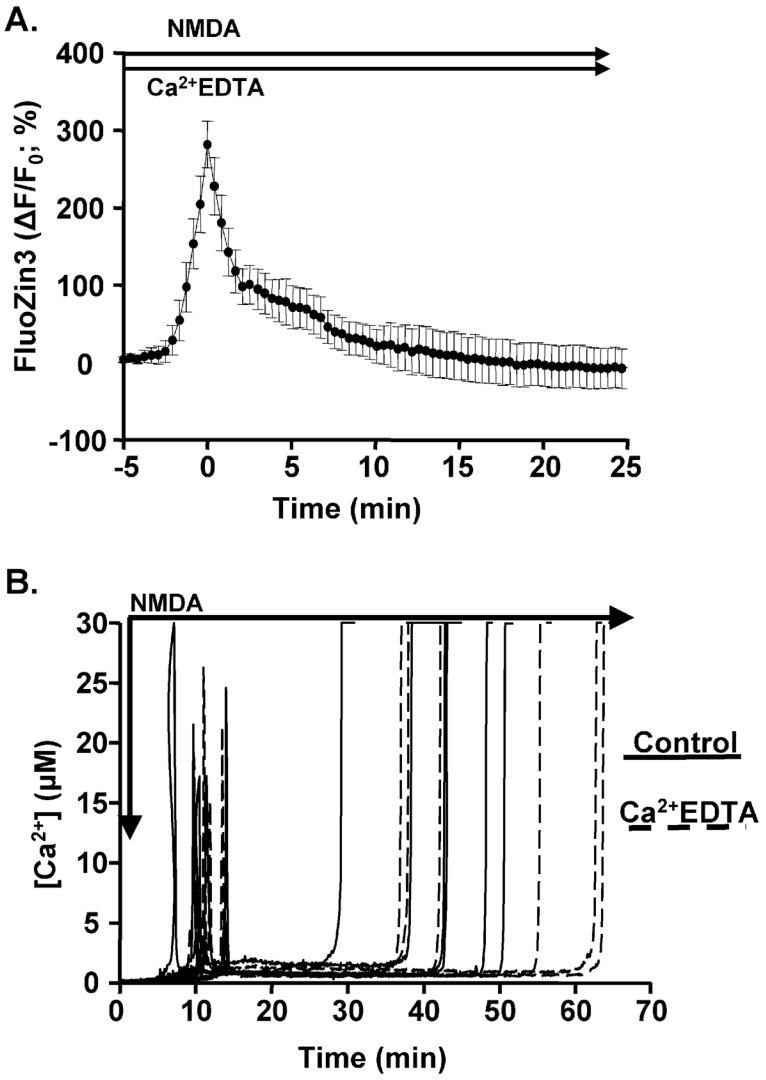

Figure 5. Ca-EDTA did not reduce initial Zn^{2+} increases, nor significantly delay the dendritic Ca^{2+} overload response

A: Slices were pre-exposed to Ca-EDTA for 20 min prior to NMDA, and the chelator was then maintained in the superfusate throughout (n=5). Initial Zn^{2+} increases were similar to those described above in control conditions (Fig 4), but on average recovered to baseline within ~15min of the peak response, unlike the plateau in normal ACSF (Fig 4). **B:** In separate experiments, compound Fura-6F responses were not modified by Ca-EDTA. Control (*solid lines*) and Ca-EDTA-treated preparations (*dashed lines*) were interleaved, and did not reveal a significant delay in arrival of Ca^{2+} overload (p=0.2; n=6 each).

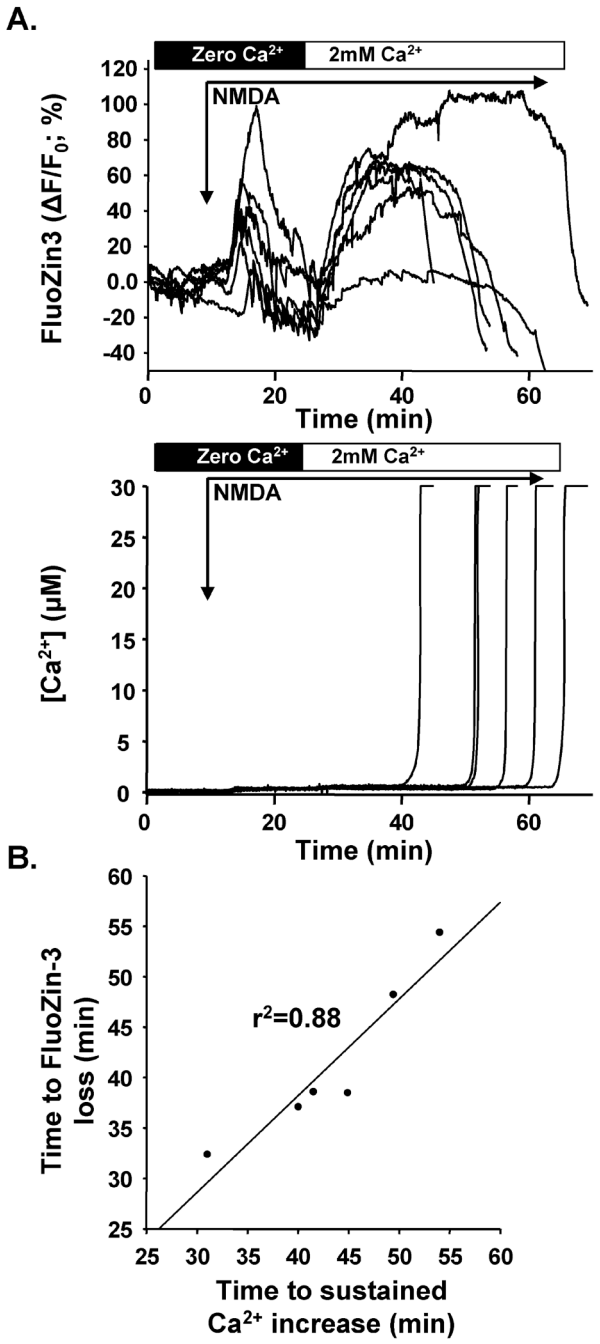

Figure 6. Effects of extracellular Ca^{2+} removal

A: Near-simultaneous FluoZin-3 (*top*) and Fura-6F (*bottom*) records from co-loaded neurons. Extracellular Ca^{2+} was washed out for 10 min before exposure to NMDA in the nominally Ca^{2+}-free solution. Subsequently 2mM Ca^{2+} was introduced 15 min into the NMDA exposure. In the nominal absence of extracellular Ca^{2+}, initial FluoZin-3 increases were reduced but not abolished (compare with Figure 4). Reintroduction of Ca^{2+} produced prompt and sustained FluoZin-3 fluorescence increases. The lower panel of A shows that Ca^{2+} removal virtually abolished Fura-6F responses, until sustained increases were observed after reintroduction of Ca^{2+}. **B:** As in control conditions, late FluoZin-3 loss was coincident with arrival of sustained Ca^{2+} increases in somata. The relationship between the time at which 50% FluoZin-3

fluorescence intensity (compared with plateau levels prior to arrival of Ca^{2+} overload) is lost is plotted against the time of half-maximal Ca^{2+} increase as the sustained Ca^{2+} response invaded somata for the 6 neurons shown in A.